

Trends in Daily Temperature and Precipitation Extremes for the Southeastern United States: 1948–2012

EMILY J. POWELL* AND BARRY D. KEIM

Department of Geography and Anthropology, Louisiana State University, Baton Rouge, Louisiana

(Manuscript received 9 June 2014, in final form 6 November 2014)

ABSTRACT

Spatial and temporal trends in temperature and precipitation extremes were investigated for the period 1948–2012 across the southeastern United States using 27 previously defined indices. Results show that regionwide warming in extreme minimum temperatures and cooling in extreme maximum temperatures occurred. The disproportionate changes in extreme daytime and nighttime temperatures are narrowing diurnal temperature ranges for most locations. The intensity and magnitude of extreme precipitation events increased overall, except for more easterly locations, particularly in South Carolina. These indices further show that warming in minimum temperatures has been pronounced most in summer and least in winter. Fall has become significantly wetter, while spring and summer have become drier, on average. Principal component analysis (PCA) was used to characterize a “geography of extremes” based on temperature and precipitation extreme indices. The PCA based on temperature indices revealed two coherent western and eastern subregions that share common modes of variability in extremes. Precipitation indices resulted in a greater number of smaller, spatially coherent groups exhibiting similar modes of variability. This classification regime illustrates important variations in extremes that exist on subregional scales. These findings have relevance for established climate research institutes, local governments, resource managers, and community planners interested in the variability of extreme events throughout the region.

1. Introduction

Impacts of extreme weather and climate events are noticeably increasing nationwide. Direct losses from natural hazards are rising ([Changnon et al. 2000](#); [Pielke et al. 2008](#)), particularly as a result of hurricanes and floods over the past 50 yr ([Gall et al. 2011](#)). Further, the number of presidentially declared disasters has substantially increased over the past 60 yr since 1953, according to Federal Emergency Management Agency (FEMA) loss statistics. While many factors play a role in determining the number of disaster declarations, such as increased social vulnerability due to more people and property in harm’s way ([Changnon et al. 2000](#); [Pielke et al. 2008](#)), direct losses from natural disasters cannot

be explained by growth in population and wealth alone. As such, the increasing national trend is likely influenced by changes in disaster frequency and magnitude, among other factors ([Gall et al. 2011](#)).

Extremes are particularly important elements of climate in the southeastern United States. Since 1980, the U.S. Southeast has been involved in more billion-dollar weather and climate disasters than any other region in the country, largely due to hurricanes, floods, and tornadoes ([NOAA 2013](#)). Although the Southeast is sometimes considered climatically homogeneous (i.e., according to the Köppen climate classification), weather patterns can vary considerably across the region ([Kunkel et al. 2013](#)). The Southeast is influenced largely by the strength and position of the Atlantic subtropical high and moisture-laden air from the Gulf of Mexico ([Henderson and Robinson 1994](#); [Henderson and Muller 1997](#)). The Bermuda high (BH) contributes to the generation of heat waves, droughts, and poor air quality, as well as steering hurricane tracks ([Kunkel et al. 2013](#)). Proximity to the Gulf of Mexico as a moisture source influences the occurrence of heavy rainfall events. The region receives heavy rainfall from midlatitude systems tracking in from

* Current affiliation: Coastal Sustainability Studio, Louisiana State University, Baton Rouge, Louisiana.

Corresponding author address: Emily Powell, Coastal Sustainability Studio, 212 Design Building, Louisiana State University, Baton Rouge, LA 70803.
E-mail: epowell8@lsu.edu

the west during winter and early spring. Heavy rainfall is also caused by cyclogenesis in the Gulf, as well as from tropical storms and hurricanes, with return periods for hurricanes averaging between 4 and 52 yr for most parts of the Gulf Coast and southern East Coast (Keim et al. 2007). Changes in the flow of the jet stream are responsible for creating stormy weather at the boundary of cold, drier air from the north and warm, moist air from the south. Strong meridional flow can result in cold-air outbreaks as far south as central Florida (Kunkel et al. 2013). The variability of extreme weather in the Southeast, combined with its diverse population composed of dense urban centers, coastal populations, and rural towns, make a more detailed analysis of extreme event behavior particularly important to the region's capacity to adapt and mitigate the adverse impacts of extreme weather and climate.

Research objectives

Impacts of climate extremes are most salient at local and regional scales (Alexander et al. 2009). Many previous studies have investigated extreme events in the Southeast (Faiers and Keim 2008; Faiers et al. 1994; Henderson and Robinson 1994; Henderson and Muller 1997; Keim 1999; Keim et al. 1995; Knight and Davis 2009), though these are independent studies that often define extremes in different ways. More comprehensive assessments of extremes in temperature and precipitation have been conducted for particular areas of the United States, including for the Northeast (Brown et al. 2010; Griffiths and Bradley 2007) and the states of New York (Insaf et al. 2012) and Utah (dos Santos et al. 2011). These studies offer a detailed analysis of the spatial and temporal variability in temperature and precipitation extremes, as well as the types of extremes most important to each region. In addition, the U.S. National Climate Assessments and synthesis products have generated more regional analyses of climate since 2000. Despite these efforts, more information regarding regional patterns of climate change and ongoing monitoring of changes in climate extremes is crucial (Griffiths and Bradley 2007; Solomon et al. 2007), particularly as changes may outpace the ability of communities to adapt and reduce adverse impacts. Kunkel et al. (2013) produced the most comprehensive assessment of Southeast climate and extremes to date in preparation for the third National Climate Assessment report (Melillo et al. 2014).

This research builds on these earlier studies by providing a detailed assessment of climate extremes for the Southeast. The objectives of this study are to 1) assess annual spatial and temporal trends in temperature and precipitation extremes from 1948 to 2012 for the Southeast, 2) examine seasonal trends in temperature and precipitation extremes, and 3) develop a regionalization of extreme variability across the region.

A comprehensive assessment of how numerous climate extremes are changing across the Southeast can provide important information for stakeholders and decision makers. For instance, information about the number of frost days, extreme wet days, length of warm spells, and changes to the growing season are important to agriculture, local infrastructure, water management, and public health (Brown et al. 2010). Additional benefits of monitoring extremes in climate using common indices include the ability to place the magnitude and frequency of extreme events in a regional, national, and global context, as well as to assess anomalous changes in extremes that may have particularly severe local impacts (Donat et al. 2013). This study contributes to regional analyses of climate change across the United States.

2. Data and methods

a. Study region

The Southeast is defined as an 11-state region (Fig. 1). This region was chosen because of its large number and variety of extreme weather and climate events that make it highly vulnerable to a changing climate (Keim 1999; Kunkel et al. 2013; NWS 2012a). Further, this region overlaps with service areas of established climate research institutes. It encompasses the six-state region of the Southern Climate Impacts Planning Program, the three-state region of the Southeast Climate Consortium, and the two-state region of the Carolinas Integrated Sciences and Assessments, which are all part of the National Oceanic and Atmospheric Administration's (NOAA) Regional Integrated Sciences and Assessments (RISA) program. These RISA teams overlap with the service areas of the Southern Regional Climate Center and Southeast Regional Climate Center. This study area also encompasses states included in the domains of the Southeast and South Central Climate Science Centers. These regional climate centers conduct applied research and develop data support and services for industry and the public aimed at increasing awareness and knowledge of climate change. A better understanding of temperature and precipitation extremes in the Southeast is integral to the work of these centers. This identical region was also used in studies by Keim (1996, 1997, 1999) and Henderson and Vega (1996).

b. Station data

This study utilizes maximum and minimum temperatures and precipitation amounts for stations included in the U.S. Historical Climatology Network (USHCN) (Menne et al. 2013). While station identifiers were pulled from what was originally part of USHCN, the data were retrieved through the Applied Climate Information

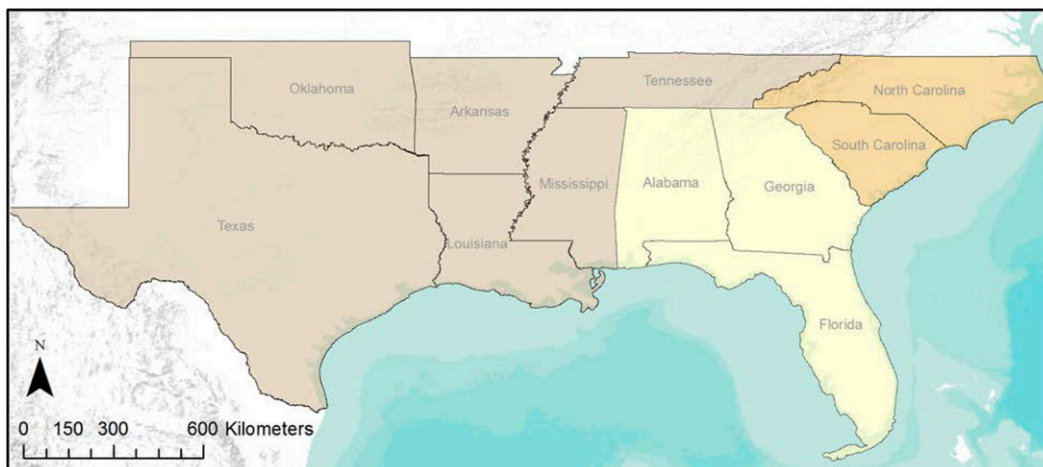


FIG. 1. The 11 states encompassing the Southeast and study area. SCIPP states are shaded in brown, SECC states are in yellow, and CISA states are in orange.

System (ACIS) (<http://rcc-acis.unl.edu>). Developed and maintained by the NOAA regional climate centers, the ACIS queries multiple datasets to obtain the best available data and high-quality station records, with highest priority given to the Global Historical Climatology Network–Daily (GHCN–Daily). The ACIS has included “replacement” values from the TD32xx datasets to account for shifts in observation times and for the generation of replacement values that failed previous quality control procedures. Preference is given to TD3210 if both TD3200 and TD3210 data are available, unlike the GHCN–Daily, which gave preference to TD3200.

Drawing from the 290 USHCN station identifiers available in this study region, 200 stations were initially selected based on a $\leq 10\%$ missing data threshold for the period 1910–2012. However, more strict criteria were used for final station selection to avoid years of missing data clustered together in certain intervals or blocks within the record, which can lead to spurious trends (Griffiths and Bradley 2007; Moberg and Jones 2005).

Final station inclusion was based on methods previously used by Moberg and Jones (2005) and Griffiths and Bradley (2007). They used a threshold of 5 missing days in 1 month for determining completeness of station records. This criterion was relaxed slightly to a threshold of 7 days to incorporate more stations while not compromising the completeness of data substantially. Final station selection criteria included the following: 1) a month was considered to have sufficiently complete data if there were 7 or fewer missing days within that month; 2) a year was considered to have sufficiently complete data if all months were complete according to criterion 1; and 3) a station was considered to have sufficiently complete data if all three of the following blocks had less than or equal to 7 missing years: 1910–44, 1945–78, and

1979–2012. This first block, 1910–44, was the most problematic with few stations having sufficiently complete data. Therefore, the start year was changed to 1948 to include a sufficient number of stations in the analysis, substantially improving the total number of stations from 38 to 107 (Fig. 2), and to correspond to the start of most daily cooperative summary of the day station records (Menne et al. 2012). While these stations do not cover all areas equally, their coverage is sufficient for purposes of this study. In addition, nearby and somewhat distant stations in the south-central United States have been shown to display similar daily patterns of extremes (Henderson and Muller 1997). We acknowledge that the choice of the 1948–2012 time series eliminates periods of extremes in the United States that occurred prior to 1948. In particular, the 1930s were marked by drought and exceptionally warm maximum and minimum temperatures (Rogers 2013; DeGaetano and Allen 2002), as well as heat waves (Kunkel et al. 2013). In addition, the Labor Day hurricane of 1935 devastated the Florida Keys with the lowest recorded pressure of any Florida hurricane at the time (Malmstadt et al. 2009), and it was one of only three hurricanes to make landfall at category 5 intensity in the United States since 1851.

c. Extreme indices

This study uses a core set of 27 indices previously developed by the Expert Team on Climate Change Detection and Indices (ETCCDI) and currently maintained through the Datasets for Indices of Climate Extremes (CLIMDEX), which produces datasets of climate extremes as a new suite of global gridded extremes products. The CLIMDEX project is a collaboration between the University of New South Wales, the University of Melbourne, the National Climatic Data Center, and

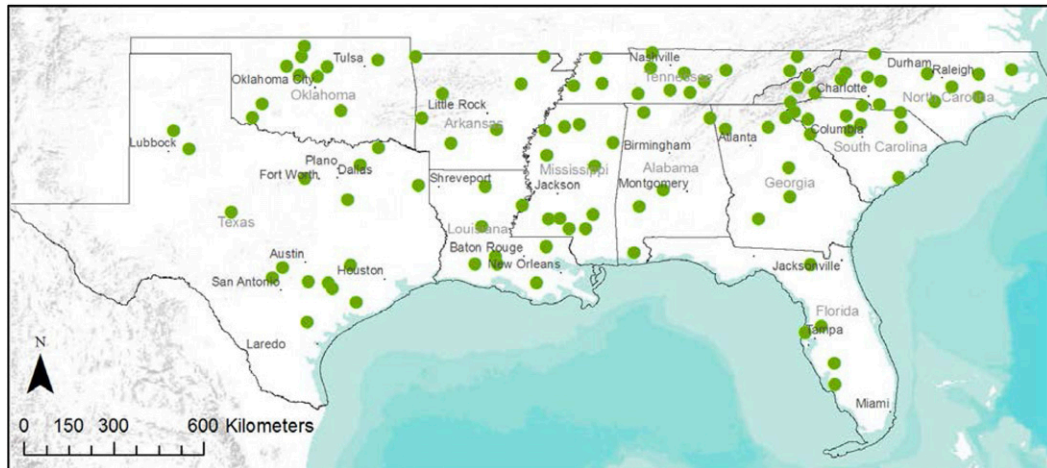


FIG. 2. Distribution of USHCN stations within the Southeast included in this analysis.

Environment Canada, and funded by the Australian Research Council's linkage project LP100200690. Headed by the World Meteorological Organization, the ETCCDI working group approved this set of extreme climate definitions as guidance for measuring and monitoring extremes, as well as related software packages for their calculations. For a description of these indices and their development, see [Donat et al. \(2013\)](#), [Alexander et al. \(2006\)](#), [Klein Tank et al. \(2009\)](#), and the CLIMDEX project website (<http://www.climdex.org>). Previous studies have applied these indices to other parts of the United States, including for the Northeast ([Brown et al. 2010](#); [Griffiths and Bradley 2007](#)), New York State ([Insaf et al. 2012](#)), and Utah ([dos Santos et al. 2011](#)). Thus, this study is part of a larger collection of efforts.

The 27 core indices include 16 temperature and 11 precipitation indices (Table 1). Temperature indices include 9 warm-related indices and 7 cold-related indices, and these can be further grouped according to their method of calculation as 4 percentile, 4 threshold, 1 absolute, and 3 duration indices. Precipitation indices include 10 wet indices and 1 dry index, which are further grouped as 2 percentile, 3 threshold, 2 absolute, 2 duration, and 2 other indices.

The CLIMDEX project maintains several software packages for the computation of these indices in different platforms. This study used the latest version, RCLimDex, which runs in R, a language and environment for statistical computing. Threshold indices were computed from a common 30-yr base period of 1981–2010 to reflect the most recent normal period. The RCLimDex program uses a bootstrapping technique to address discontinuities in the expected rates for the years on the boundaries of the base period, thereby making estimations of threshold exceedance rates for both the in-base and out-of-base periods comparable and temporally consistent ([Zhang](#)

et al. 2005). See [Zhang et al. \(2005\)](#) and [Zhang and Yang \(2004\)](#) for a description of the bootstrapping procedure used to calculate the base period thresholds.

The RCLimDex program allows for several user-defined inputs when calculating indices. Default temperature thresholds are automatically computed for summer days (25°C), tropical nights (20°C), frost days, (0°C), and ice days (0°C). In addition to these default values, user-defined thresholds produce additional estimates of these indices, as well as one precipitation index, that can better reflect the region under investigation. In addition to the core indices, the program calculates monthly and annual mean maximum and minimum temperatures. This yields a total of 33 indices.

The following thresholds were used in this study in addition to default values:

- (i) an upper threshold of daily maximum temperature of 35°C (95°F);
- (ii) upper threshold of daily minimum temperature of 24°C (75°F);
- (iii) lower threshold of daily maximum temperature of -2°C (28°F);
- (iv) lower threshold of daily minimum temperature of -2°C (28°F); and
- (v) daily precipitation threshold of 102 mm (4 in.).

These values were chosen for consistency with other work ([Melillo et al. 2014](#); [Kunkel et al. 2013](#)) and because they more appropriately analyze extremes in the climate of this region, which is generally warmer than much of the United States. The lower threshold of -2°C for daily maximum and minimum temperatures was chosen to assess the occurrence of hard freezes in addition to frost days and ice days that are based on

TABLE 1. List of the ETCCDI's (a) 16 core extreme temperature indices and (b) 11 core extreme precipitation indices and their definitions (available online at <http://www.climdex.org/indices.html>).

(a) Temperature indices			
Index name	ID	Definition	Units
Percentile			
Warm days	TX90p	% of days when Tmax is > 90th percentile	%
Warm nights	TN90p	% of days when Tmin is > 90th percentile	%
Cool days	TX10p	% of days when Tmax is < 10th percentile	%
Cool nights	TN10p	% of days when Tmin is < 10th percentile	%
Threshold			
Summer days	SU25	Annual count when Tmax > 25°C	days
Tropical nights	TR20	Annual count when Tmin > 20°C	days
Ice days	ID0	Annual count when Tmax < 0°C	days
Frost days	FD0	Annual count when Tmin < 0°C	days
Absolute			
Warmest day	TXx	Annual maximum value of daily max temperature	°C
Warmest night	TNx	Annual maximum value of daily min temperature	°C
Coldest day	TXn	Annual minimum value of daily max temperature	°C
Coldest night	TNn	Annual minimum value of daily min temperature	°C
Diurnal temperature range	DTR	Daily Tmax – Daily Tmin	°C
Duration			
Growing season length	GSL	Annual count between first span of at least 6 days with Tmean > 5°C and first span after 1 Jul of 6 days with Tmean < 5°C	days
Warm spell duration	WSDI	Annual count of days with at least 6 consecutive days when Tmax > 90th percentile	days
Cold spell duration	CSDI	Annual count of days with at least 6 consecutive days when Tmin < 10th percentile	days
(b) Precipitation indices			
Percentile			
Precipitation on very wet days	R95pTOT	Annual total precipitation (PRCP) when RR > 95th percentile	mm
Precipitation on extremely wet days	R99pTOT	Annual total PRCP when RR > 99th percentile	mm
Threshold			
No. of heavy precipitation days	R10mm	Annual count of days when PRCP ≥ 10 mm	days
No. of very heavy precipitation days	R20mm	Annual count of days when PRCP ≥ 20 mm	days
No. of days above <i>nn</i> mm	Rnnmm	Annual count of days when PRCP ≥ <i>nn</i> (user-defined threshold)	days
Absolute			
Max 1-day precipitation	Rx1day	Annual max 1-day precipitation	mm
Max 5-day precipitation	Rx5day	Annual max consecutive 5-day precipitation	mm
Duration			
Consecutive wet days	CWD	Max number of consecutive days when RR ≥ 1 mm	days
Consecutive dry days	CDD	Max number of consecutive days with RR < 1 mm	days
Other			
Annual total wet day precipitation	PRCPTOT	Annual total PRCP in wet days (RR ≥ 1 mm)	mm
Simple daily intensity index	SDII	Annual total precipitation divided by the number of wet days (PRCP ≥ 1 mm)	mm day ⁻¹

minimum and maximum temperature thresholds of 0°C, respectively. The choice of daily precipitation threshold of 102 mm was based on [Melillo et al. \(2014\)](#), which informed the third National Climate Assessment. Further, the other precipitation indices use thresholds that represent relatively low magnitudes and a much higher threshold was desired to reflect heavy rainfall events more characteristic of the region, which can exceed

100 mm in a 24-h period ([Faiers and Keim 2008](#); [Keim 1999](#)). These user-defined values were kept consistent across the study region to more easily compare and analyze spatial variations in extremes. Seasonal trends were calculated for a subset of indices where both monthly and annual values are available in the RClimDex program.

In addition to manual checks for data completeness, quality control tests for completeness and erroneous

data are embedded in the RClimDex program. The program calculates annual values for all 33 indices and monthly values for 13 indices. Monthly values are calculated for all months with no more than 3 missing days, and annual values are calculated for years with no more than 15 days of missing data. For threshold indices, data must be at least 70% complete (Zhang and Yang 2004). These missing-day criteria are stricter than the manual checks for station completeness described above; thus, missing values do occur in these records. The software also identifies outliers in daily maximum and minimum temperatures, represented as the mean plus or minus n times the standard deviation of the value for the day. This study used a value of four standard deviations to flag outliers to be consistent with previous work (Brown et al. 2010) and the RClimDex user manual (Zhang and Yang 2004). Any outliers identified in the data were not changed since this study was interested in detecting extreme values. The RClimDex program defines unreasonable values in the daily data as negative daily precipitation amounts and daily maximum temperatures less than daily minimum temperatures. Negative precipitation values and maximum temperatures less than minimum temperatures were changed to missing values. If the difference between the daily maximum and minimum temperature was zero, the value was left unchanged.

Despite these quality control checks embedded in the software, additional bias and inhomogeneity adjustments were not made. The lack of bias adjustments and issues of inhomogeneity represent a limitation of these data. Particularly, changes associated with a station's location, sensor, and time of observation can introduce spurious trends and bias in the annual series. Daily precipitation data were not adjusted for inhomogeneities because of the complexities involved and a lack of reliable methods in correcting precipitation data (Brown et al. 2010). Additionally, the number of stations included in this study made correcting temperature data for inhomogeneities unfeasible. Metadata for all stations included here are available through the National Climatic Data Center (NCDC) Historical Observing Metadata Repository (<http://ncdc.noaa.gov/homr>). Station relocations were documented for all 107 stations over the 65-yr period. Most station relocations remained within the National Weather Service's guidelines of 5 miles per 100 feet (NWS 2012b). While a handful of relocations exceeded these thresholds, stations maintained their station IDs; thus, changes were deemed climatologically compatible (NWS 2012b).

The RClimDex program uses linear regression for trend calculations. Previous studies that applied these same ETCCDI indices to other regions of the country used ordinary least squares (OLS) regression to assess

trends in these extremes (Brown et al. 2010; Griffiths and Bradley 2007; Insaf et al. 2012). While the OLS method of trend fitting is the most widely used and accepted method for linear regression (Griffiths and Bradley 2007), it is sensitive to outliers and non-Gaussian distributions (Brown et al. 2010). Despite its limitations, the OLS regression was used in this study to remain consistent with similar work. The RClimDex software produces time series and computes trend lines by linear least squares and locally weighted linear regression using a loess smoother function in R (Zhang and Yang 2004). Significance is based on the t test for the estimate of the slope at the 95% level (p value < 0.05). All index calculations and statistical analyses were conducted in R (<http://www.R-project.org>). Thematic maps were produced in ArcMap 10 to reflect spatial trends in each index.

Principal component analysis (PCA) was used to further characterize the variability in extreme indices and develop a regionalization of extremes. S-mode PCAs were used for both temperature and precipitation extreme indices to group stations that have experienced similar temporal patterns in extremes over the 65-yr record. Input matrices consisted of stations as the variables (i.e., columns) and years as the individuals (i.e., rows). This yielded a temperature (precipitation) matrix of 107 columns by 65 rows, with the common variable under investigation being average annual temperature (precipitation) index values for each station. Raw index values were standardized to enable the synthesis of multiple indices with different units and ensure each index would be represented equally in the PCA. For each index, annual z scores were calculated by subtracting the mean from the annual index value and dividing the result by the standard deviation, as follows:

$$Z_{ij} = \frac{(I_{ij} - \mu_i)}{\sigma_i},$$

where Z is the standardized value (or z score) for index i and year j ; I is the raw annual index value for index i and year j ; μ is the mean for the period of record and index i ; and σ is the standard deviation for the period of record and index i . This formula was applied to all 33 indices and all 107 stations. Finally, for each station, annual z scores for all temperature and precipitation indices were averaged together to derive a single value for each station and year. Thus, the two input matrices were based on the average of 22 temperature and 11 precipitation indices.

Datasets containing missing values can be problematic in a PCA. To address missing values and avoid removal of data used in the PCA, missing values were imputed using functions available in the "missMDA" package

in R. The “`estim_ncpPCA`” function was used to estimate the number of dimensions or components that should be used to replace missing values with predicted ones. The generalized cross-validation criteria was applied to identify the number of components that produces the smallest mean square error of prediction for use in the imputation procedure, as this method provides a straightforward way to estimate the number of dimensions without being computationally intensive (Josse and Husson 2012). This value was used as input to the imputation procedure, using the “`imputePCA`” function. This imputation function in R imputes missing values using the mean of each variable. While the mean substitution or imputation method is a common approach for handling missing values (Karhunen 2011), it substitutes the same value for each missing data point, which can artificially reduce the variance in the variable. However, if the dataset contains only a limited number of missing data points and those missing data points are spread out, then the replacement of missing values with the mean would not have as large of an effect on the variance. In fact, when the percentage of missing data is small, replacing the missing values with the mean is a common strategy in multivariate statistics (Dodge 1985). Both temperature and precipitation datasets contained a relatively small percentage of missing data, roughly 6%, and the mean substitution method was considered nonproblematic.

Finally, varimax rotation was applied for comparison with unrotated components. Varimax rotation is a widely used orthogonal rotation method that attempts to polarize loadings so that they are high or low, making it easier to connect factors with variables for interpretation (Hamilton 1992) and identify a subset of variables that covary in a similar way (Richman 1986). Despite the fact that orthogonally rotated solutions may be less stable than oblique rotations, thereby producing less consistent results (White et al. 1991), most climatological studies employ a correlation matrix and varimax rotation (Green et al. 1993; Nogueira et al. 2013; Vega and Henderson 1996). Moreover, varimax rotation is widely accepted as being the most accurate analytic technique for orthogonal rotation when a priori knowledge of a dataset exists (Richman 1986).

3. Results

a. Regionwide trends

The direction of trends for temperature-related indices may initially seem contradictory, but the trends are complimentary and consistent (Fig. 3). The preponderance of evidence suggests that warming in recent decades can be attributed more to increases in daily

minimum rather than daily maximum temperatures. The majority of stations show negative trends in maximum temperature-related indices, including summer days (above 25° and 35°C), percentage of days above the 90th percentile, and warm spells. Conversely, positive trends are generally observed in minimum temperature-related indices, including tropical nights (above 20° and 24°C), warmest nights, and percentage of days with minimum temperatures above the 90th percentile. About 74% of stations show increases in tropical nights above 24°C, and 45% of stations are significant. Roughly 67% of stations show decreases in summer days above 35°C, with 16% being significant. As a result, the majority of stations (57%) show significant decreasing trends in the diurnal temperature range index. Overall, duration indices (i.e., warm and cold spells) exhibit more significant negative than positive trends, indicating that severe extreme heat and cold outbreaks became increasingly shorter between 1948 and 2012: a trend that, if continued, may help counteract any increases in their intensity.

In general, wet-related indices suggest that the frequency and intensity of precipitation events increased in the Southeast. Wet-related indices show more significant positive than significant negative trends; however, considerably fewer significant trends exist overall compared to temperature-related indices. For instance, about 77% of stations showed increases in the amount of precipitation on very wet days (>95th percentile), but only about 10% of these trends were significant; 72% of stations show increases in the number of very heavy precipitation days, with only 9% being significant. The simple daily intensity index (SDII) shows the greatest significance, with 75% of locations showing upward trends in this index and 25% being significant. This indicates that precipitation events became increasingly efficient during this 65-yr period. While the frequency and intensity of extreme events generally increased, evidence suggests that extreme precipitation appears to be getting shorter in duration. The wet and dry spell indices [consecutive wet days (CWD) and consecutive dry days (CDD)] suggest shorter wet and dry spells across the Southeast, with more significant negative than positive trends. In fact, 72% of stations exhibited downward trends in the CWD index, with 17% of these being significant, compared to 25% of stations showing upward trends in this same index, with only 1% being significant.

Subregional differences exist across the Southeast. The majority of stations in Texas and Oklahoma showed increasing wet trends during this period and significant trends were all positive, excluding duration indices. In particular, all stations in Oklahoma experienced upward trends in the following indices: amount of rainfall on

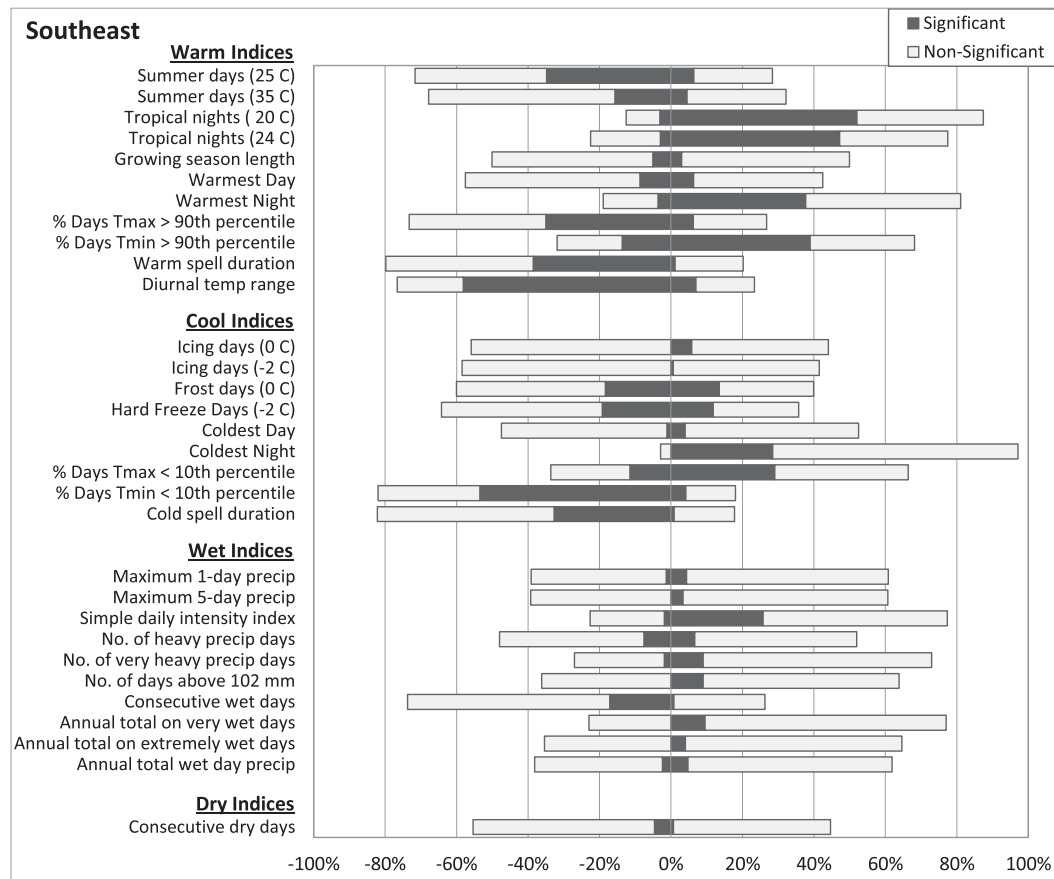


FIG. 3. Percentage of stations in the Southeast showing positive and negative trends in extreme indices from 1948 to 2012 [image concept borrowed from [Insaf et al. \(2012\)](#)]. The percentage of stations with positive or negative trends is shown by the length of the bar to the right or left of the zero line, respectively.

very wet days (R95p), number of heavy precipitation days, and annual total precipitation (PRCPTOT) (Fig. 4). Conversely, South Carolina became much drier (Fig. 5). It is the only state in the region where the majority of locations experienced downward trends in every wet index, with a corresponding increase in dry spells (CDD).

b. Spatial trends in temperature extremes

Annual trends were mapped to examine spatial patterns in these indices across the Southeast. Spatial trends in warm and cold temperature-related indices are shown in Figs. 6 and 7, respectively. A red symbol represents a trend toward a warmer climate; a blue symbol denotes a trend toward a cooler climate. These may be positive or negative trends, depending on the given index. Larger circles indicate significance at the 5% (largest) or 10% (medium) levels; smallest circles represent nonsignificant trends.

Resulting spatial patterns reaffirm that warming has not been a universal component of the Southeast since the mid-1900s. Most stations experienced downward trends in extreme maximum temperatures. Figure 6c

shows regionwide decreases in the number of summer days above 35°C for most locations, with some exceptions in Louisiana and southern Mississippi, Florida, Georgia, and the western Carolinas. Further evidence of daytime cooling was observed in warm days (Fig. 6a), as well as in warmest days, barring Louisiana and the northern Gulf Coast (Fig. 6e). Similarly, regionwide decreasing trends were observed in the warm spell duration index, with many trends significant at the 5% level (Fig. 6h). Conversely, extreme minimum temperatures have been increasing for most stations. Figure 6d shows regionwide increases in the number of tropical nights above 24°C, with many trends significant at the 5% and 10% levels. Further, most locations exhibit upward trends in warm nights above the 90th percentile (Fig. 6b) and in the warmest nights (Fig. 6f). Some indices showed less spatial coherence and exhibited fewer significant trends, such as warmest days (Fig. 6e) and growing season lengths (Fig. 6g).

Trends in cold temperature-related indices and the diurnal temperature range are shown in Fig. 7. Trends in

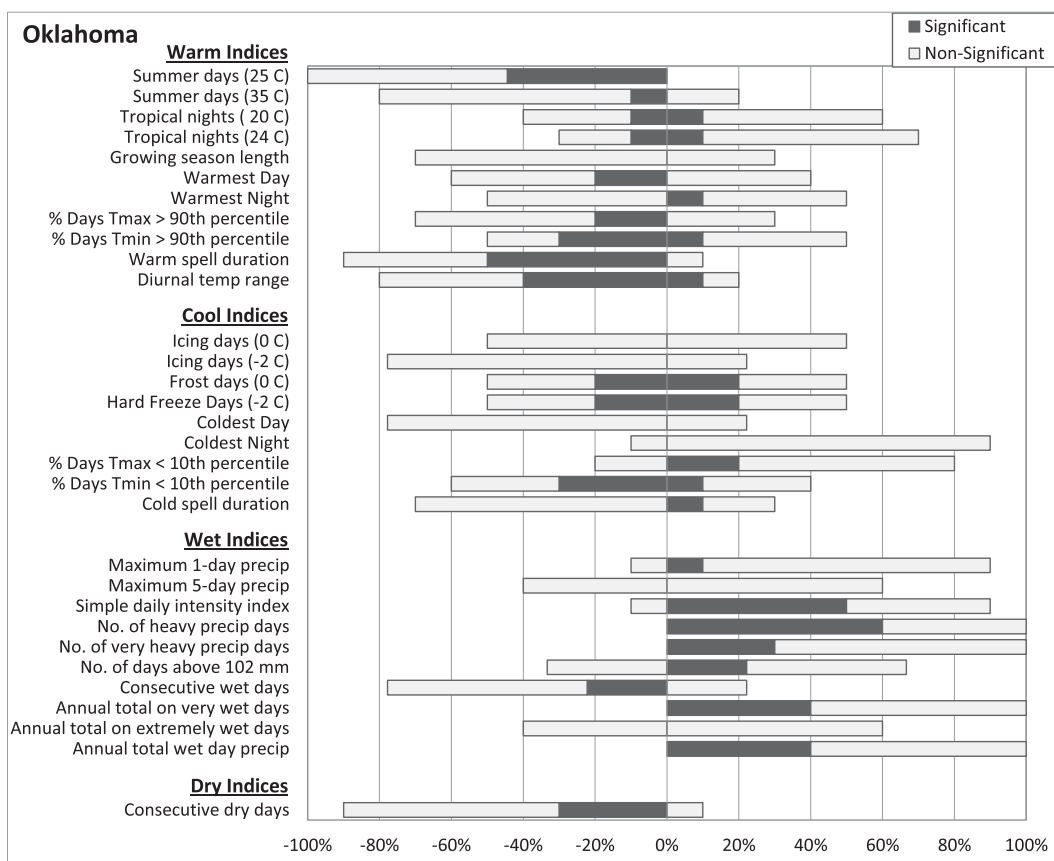


FIG. 4. Percentage of stations in Oklahoma showing positive and negative trends in extreme indices from 1948 to 2012 [image concept borrowed from [Insaf et al. \(2012\)](#)]. The percentage of stations with positive or negative trends is shown by the length of the bar to the right or left of the zero line, respectively.

these indices further complement those observed in warm-related indices, with daytime cooling and nighttime warming apparent in several indices. Many locations saw upward trends in the percentage of cool days, though significant downward trends exist as well (Fig. 7a). Conversely, the majority of stations show significant downward trends in the percentage of cool nights (Fig. 7b). Regionwide significant upward trends in coldest nights exist, meaning that absolute coldest nighttime temperatures became warmer year after year, barring the extreme southeast portion of the region and Oklahoma, where trends were largely positive but nonsignificant (Fig. 7f). Finally, diurnal temperature ranges (DTR) significantly decreased across the region, with few exceptions in more northerly locations (Fig. 7h). In general, trends in the number of ice days are not significant, with the exception of significant positive trends in Arkansas and North Carolina (Fig. 7c). Significant trends in frost days vary, though the region appears to have seen increasingly fewer frost days overall during this period (Fig. 7d).

Results from the PCA returned 65 components that together explain all of the variance in the original set of stations. The standard deviations of the eigenvalues, proportion of variance, and cumulative proportions of variance for the first 30 components were examined to determine the number of components to retain. Based on the “above one” criterion and analysis of the scree and bar plots of the eigenvalues, the first two components were retained, which together explained 65% of the total variance in temperature extreme indices for these stations. Figure 8 shows the signs of the coefficients for the first two components retained for analysis. Based on unrotated components, the first component (PC1) suggests that all stations share a common mode of variability, while PC2 divided the stations into eastern and western subregions. Rotated components further partitioned the Southeast into western and eastern subregions. As rotation maximizes loadings onto a particular component, stations without a positive or negative sign were zero or near zero for that component. These results suggest that eastern stations share a common mode of variability,

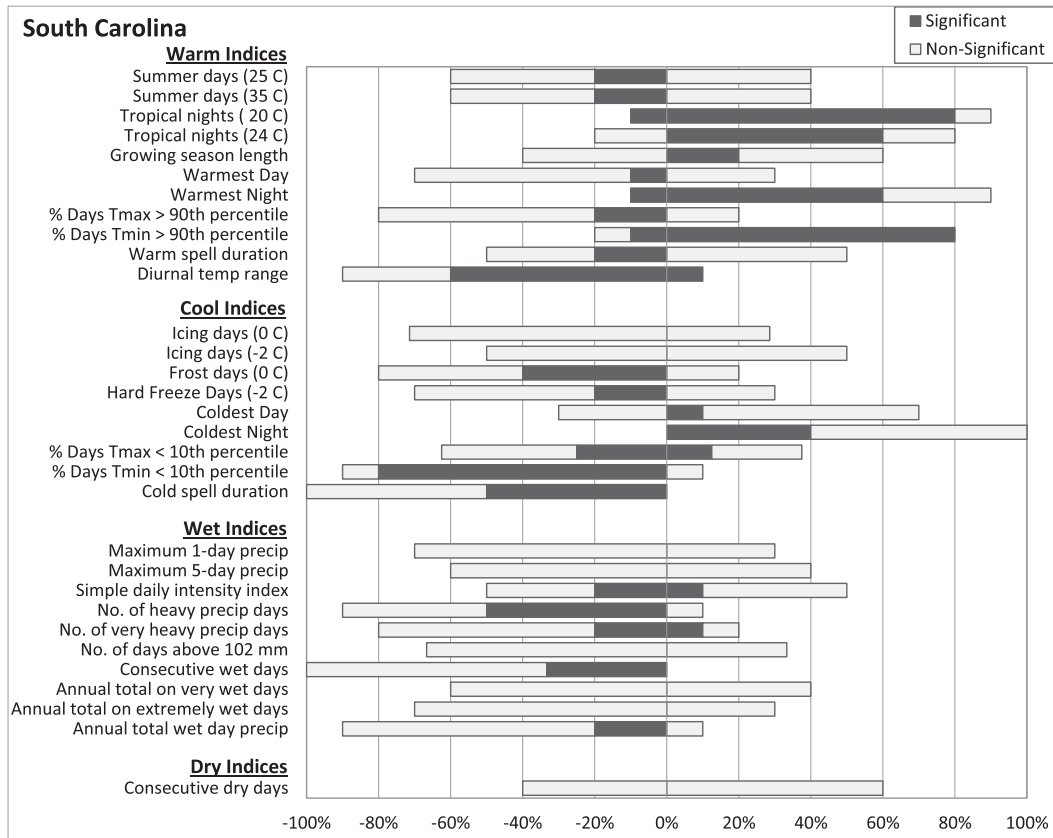


FIG. 5. Percentage of stations in South Carolina showing positive and negative trends in extreme indices from 1948 to 2012 [image concept borrowed from [Insaf et al. \(2012\)](#)]. The percentage of stations with positive or negative trends is shown by the length of the bar to the right or left of the zero line, respectively.

while more westerly stations share a common mode of variability. This classification regime may be at least partially explained by the scale of the region being investigated. The Southeast, as defined here, closely matches the scale at which synoptic weather patterns occur. The positioning of the BH and increased meridional flow of the jet stream can create large swings in temperatures in the region, as cold air from the north plunges southward and warm Gulf air is carried farther north. As low pressure and associated frontal systems move east through the region from the west, warm extremes often develop under a ridge of high pressure ahead of the cold front to the east, and cold extremes can occur near the trough behind the cold frontal boundary farther west. Thus, this east–west dichotomy may be explained by this typical synoptic weather pattern that can impact the region throughout the year.

c. Spatial trends in precipitation extremes

Precipitation-related indices were mapped to similarly show spatial patterns in precipitation extremes across the Southeast. Green circles denote increasing wetness, while brown circles denote drying trends. The

size of the circles represents significance, similar to that used for temperature indices. [Figure 9](#) shows results of the precipitation indices that are in units of millimeters, which include percentile and absolute indices. [Figure 10](#) shows precipitation indices in units of days, which include threshold and duration indices. Precipitation indices show less spatial coherence overall, and it is not uncommon for nearby locations to show opposite trends in the same precipitation indices, suggesting greater spatial variability across the region.

Despite fewer significant trends overall, evidence suggests that much of the Southeast saw significantly more extreme precipitation. According to the SDII, precipitation events have become more efficient, or intense, across the region ([Fig. 9f](#)). This is particularly evident in eastern Texas, Oklahoma, much of Louisiana and Mississippi, southern Georgia, Florida, and parts of Tennessee. This is further supported by regionwide decreasing trends in wet spells, with many trends significant at the 5% level ([Fig. 10d](#)).

A distinct east–west pattern is evident in several indices, whereby increasing dryness is observed in the east

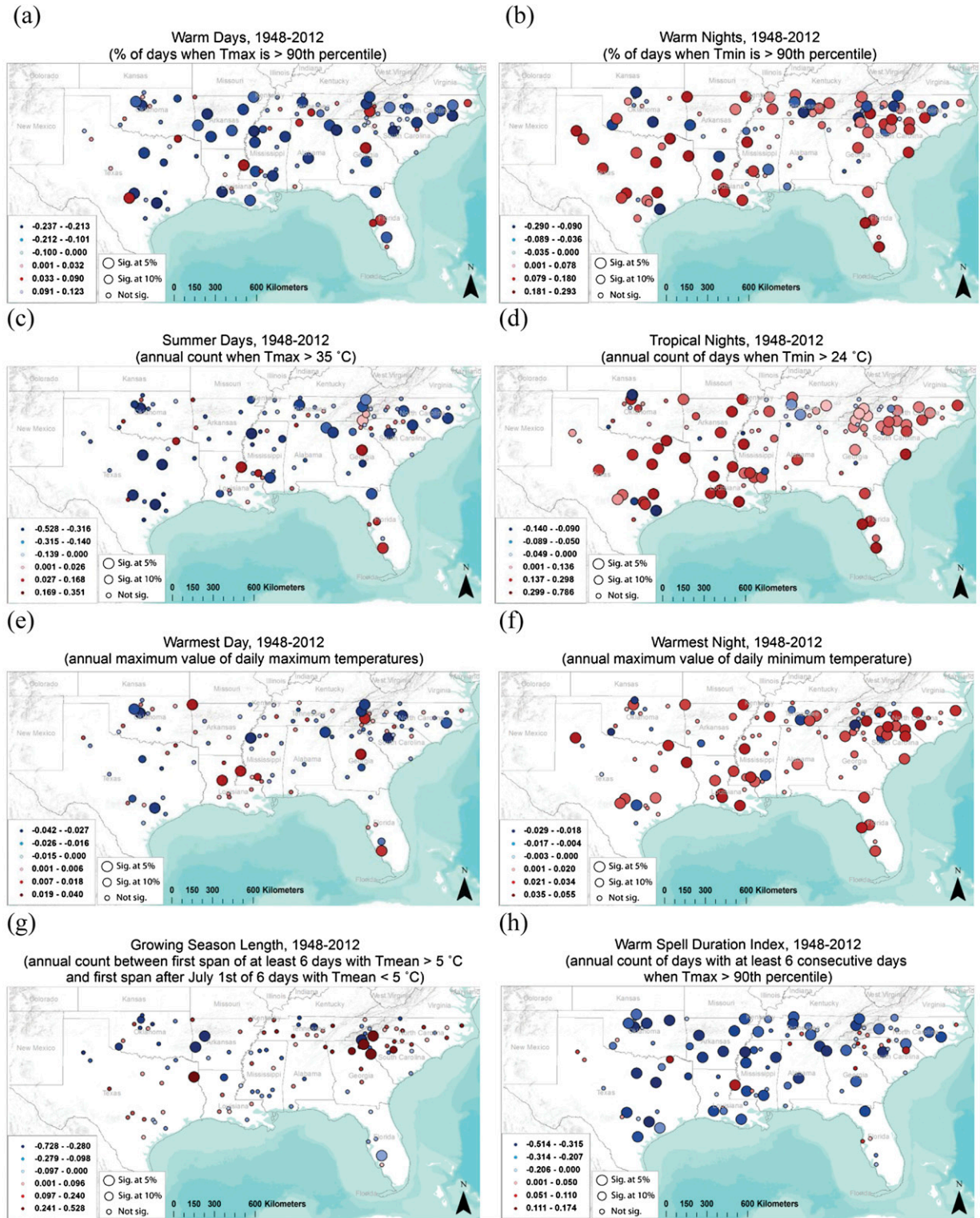


FIG. 6. Trends in warm temperature extreme indices for the Southeast from 1948 to 2012. The largest sized circles are significant at the 0.05 level, medium sized circles are significant at the 0.10 level, and the smallest circles are nonsignificant.

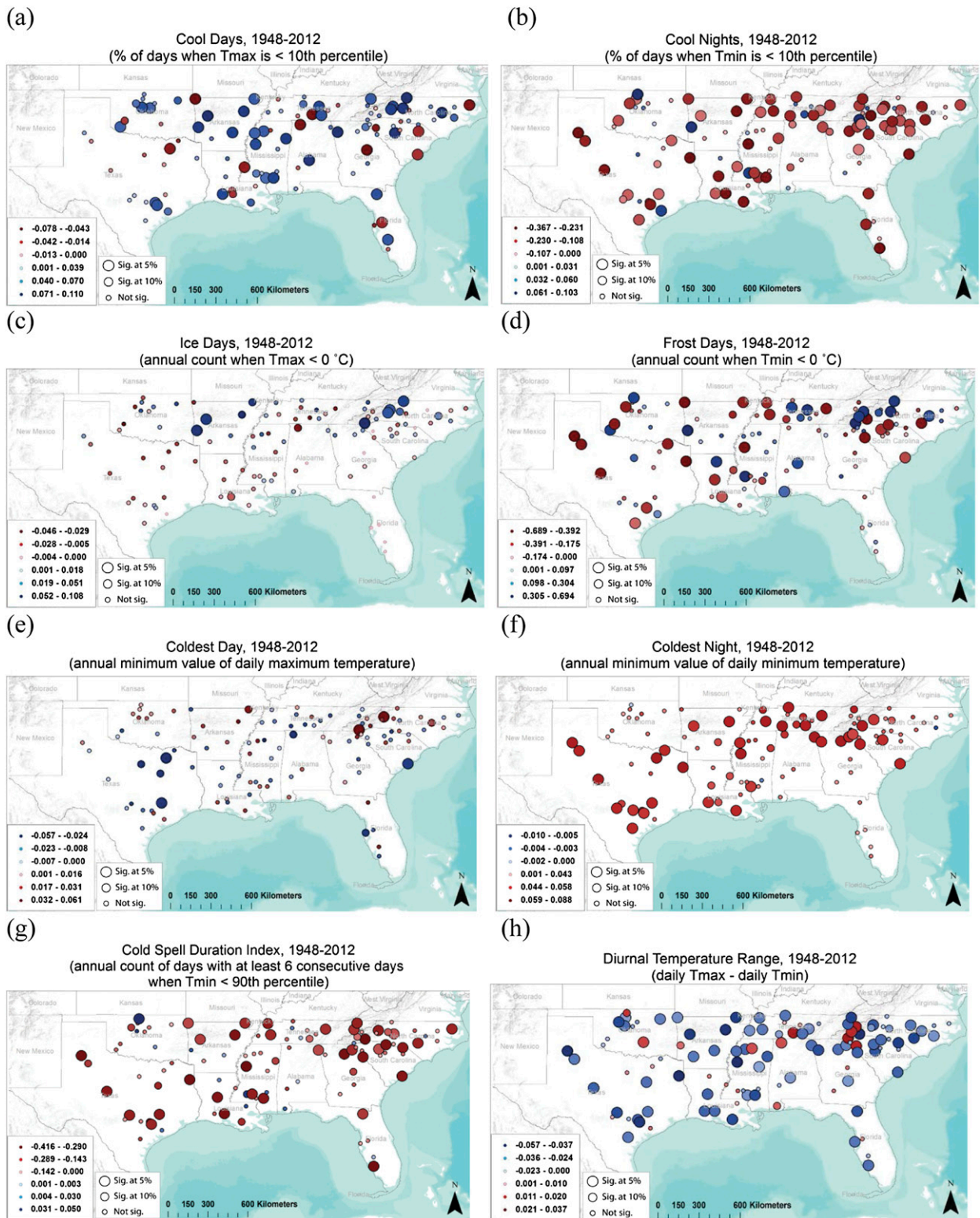


FIG. 7. Trends in cold temperature extreme indices for the Southeast from 1948 to 2012. The largest sized circles are significant at the 0.05 level, medium sized circles are significant at the 0.10 level, and the smallest circles are nonsignificant.

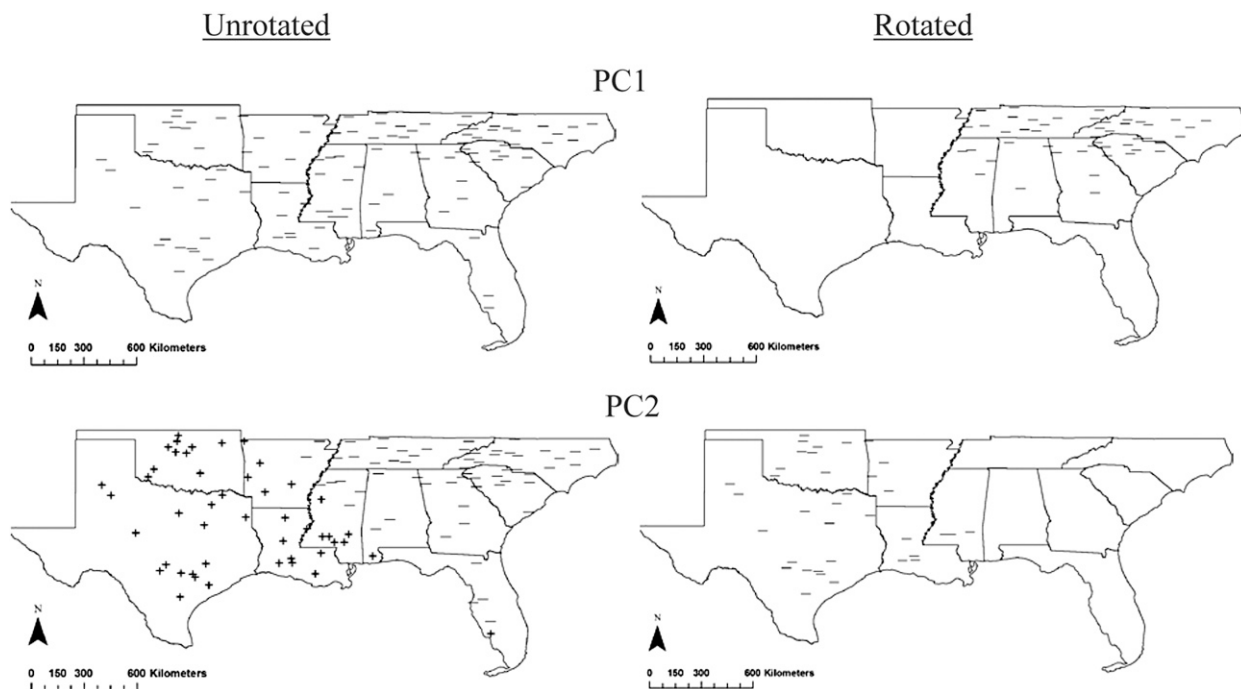


FIG. 8. Signs of the coefficients for the first and second principal components, PC1 and PC2, of extreme temperature indices in the Southeast: (left) unrotated components and (right) varimax rotated components.

and increasing wetness is observed in central and western portions of the region. This pattern is especially evident in annual total precipitation (Fig. 9e); number of heavy (≥ 10 mm) and very heavy (≥ 20 mm) precipitation days (Figs. 10a,b, respectively); and, to a lesser extent, the SDII (Fig. 9f). Other precipitation indices show greater spatial variability and fewer significant trends, including precipitation on very wet days (Fig. 9a) and extremely wet days (Fig. 9b), extreme precipitation days (Fig. 10c), and annual maximum 1-day and consecutive 5-day precipitation (Figs. 9c,d, respectively).

Though drought is a common phenomenon in this region, particularly in the west, few significant upward trends in CDD are observed (Fig. 10e). The few significant trends that exist reflect shorter, not longer, dry spells in Oklahoma and the surrounding stations in western Arkansas and northern Texas. Similar to previous research that has shown no clear trends in drought across the United States (Easterling et al. 2000), the CDD exhibits no clear spatial trend to indicate whether droughts increased or decreased across the region. However, the CWD index suggests that wet spells became shorter for most stations (Fig. 10d). These duration indices should be compared to other drought-related indices to investigate what different metrics reveal about drought and precipitation regimes across the region.

An S-mode PCA was used to further assess variability in these 11 extreme precipitation indices. Unlike the

PCA results based on temperature indices, a few components could not account for the majority of variance in the precipitation indices. The first three components resulting from the PCA accounted for only 37% of the total variance. Following the strict above one criterion, 10 components were retained. This criterion was compared against the scree and bar plots, which showed no major cutoff in the data after PC1. In addition, there was very little change in the amount of variance explained by each additional component beyond PC10. These first 10 components explain 62% of variance in the original data, and it may be worth noting that it would require retaining 30 components to explain 88% of the total variance in these indices.

Figure 11 shows the signs of the coefficients for the first five components. Unrotated components showed evidence of classic Buell sequencing patterns [see Buell (1975) and Richman (1986) for a description]. Given the possibility of domain shape dependence inherent in unrotated components, rotated components may provide a more reliable regionalization of precipitation extremes. Varimax rotation revealed a very different regionalization of extremes than that shown by unrotated components. In particular, rotation yielded a greater number of small groups of stations clustered together across the region. Thus, only nearby stations tend to exhibit similar modes of variability, and stations with similar variance in precipitation extremes are

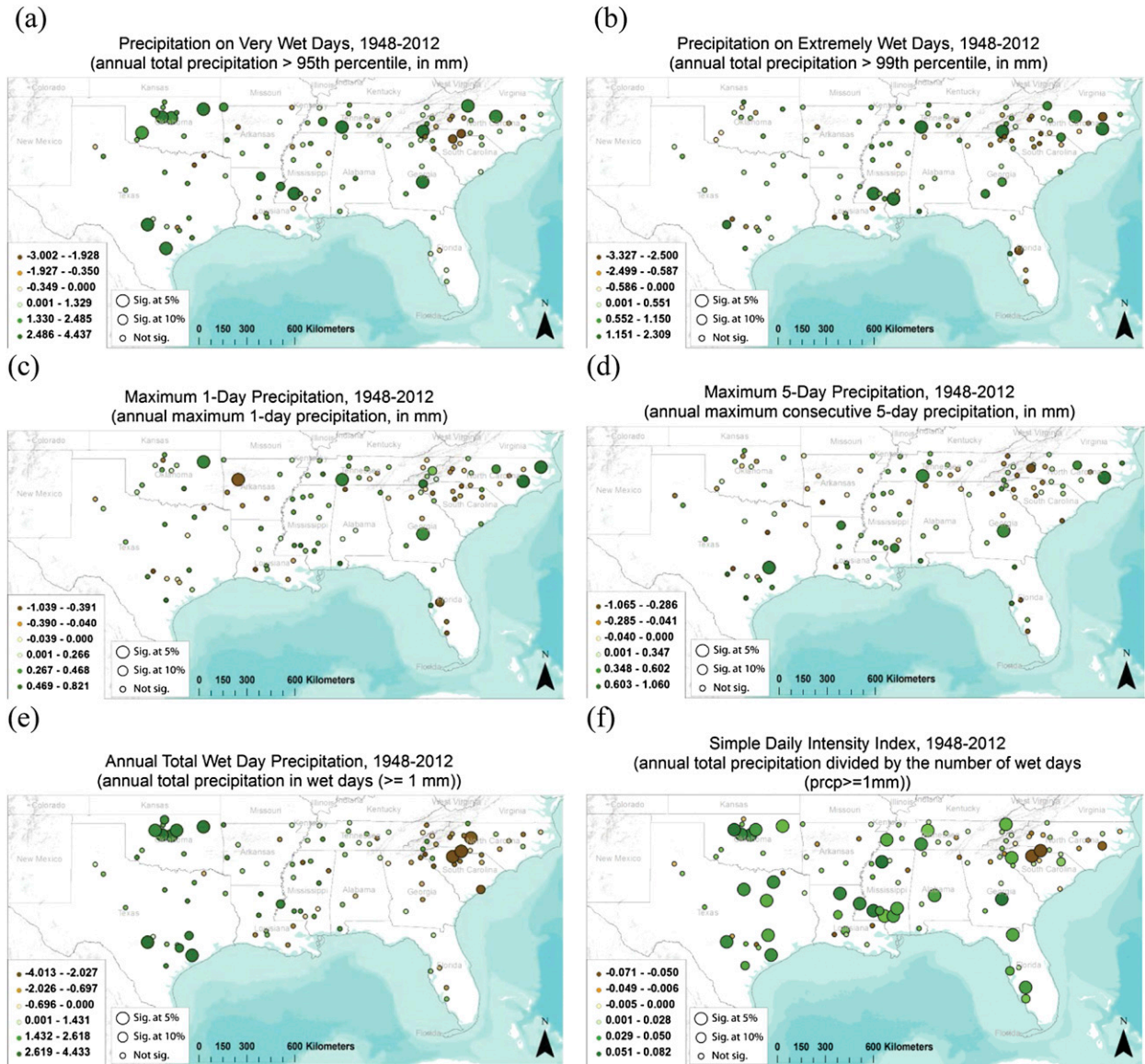


FIG. 9. Trends in percentile and absolute precipitation extreme indices, in units of millimeters [mm day^{-1} for (f)] for the Southeast from 1948 to 2012. The largest sized circles are significant at the 0.05 level, medium sized circles are significant at the 0.10 level, and the smallest circles are nonsignificant.

generally clustered together. Further, the need to retain more components to explain about the same amount of variance in the data as for temperature extremes suggests that precipitation extremes exhibit much greater variability than temperature extremes. Thus, a PCA may be less successful overall in explaining the variability in precipitation extremes in this region.

d. Temporal trends

Time series data illustrate how extremes in maximum versus minimum temperatures changed from 1948 to 2012 for the region as a whole (Fig. 12). These time

series reflect annual averages in summer days and tropical nights for all 11 states in the study region, with the least squares trend line. While previous research has revealed similar trends in maximum and minimum temperatures for the region, these time series exemplify the differing trends that exist between extreme maximum and minimum temperatures. Little change or a slightly decreasing trend occurred in the frequency of extremely hot days. This trend is dominated by a peak in summer days in the 1950s corresponding to a period of extremely dry weather (Kunkel et al. 2013), when roughly 80% of the U.S. Southeast and South (as defined

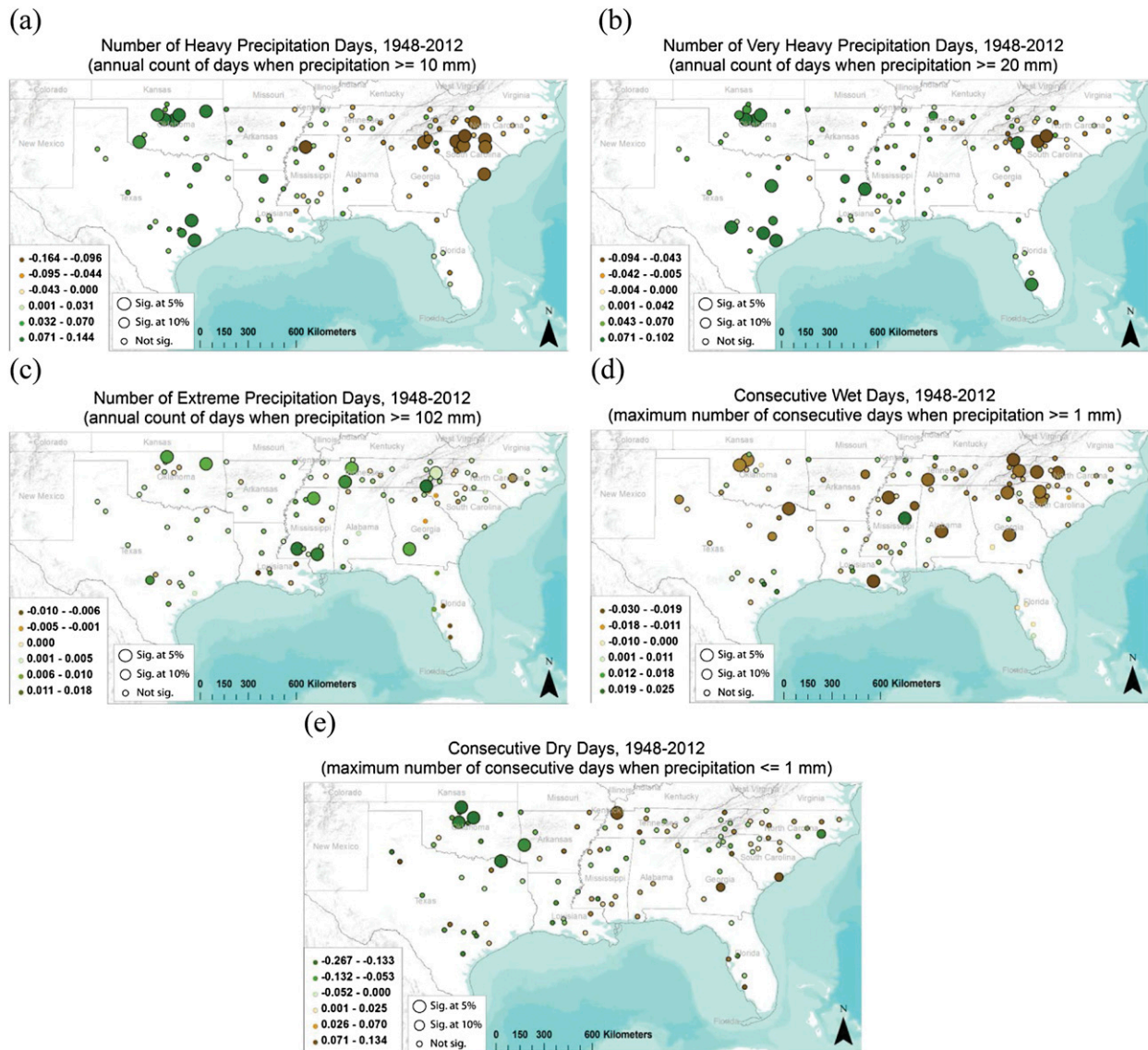


FIG. 10. Trends in threshold and duration precipitation extreme indices, in units of days, for the Southeast from 1948 to 2012. The largest sized circles are significant at the 0.05 level, medium sized circles are significant at the 0.10 level, and the smallest circles are nonsignificant.

by NCDC's climate extreme index) were affected by severe or extreme drought. A second peak occurred in the 2000s when roughly 40% of the Southeast and South were in drought (Easterling et al. 2000). Another peak is evident in the 1980s. Despite similar peaks in the frequency of tropical nights during the early, middle, and latter parts of the record, a much greater increasing trend exists overall in tropical nights, particularly since the 1980s. These results are consistent with DeGaetano and Allen (2002), who found that century-long trends in warm temperature extremes for both maximum and minimum temperatures peaked in the 1930s, 1950s, and

1980s, coinciding temporally and spatially with widespread drought episodes.

Summer days have occurred much more frequently than tropical nights, though these indices suggest that tropical nights have become as frequent as summer days. However, these trends do not necessarily mean they will continue into the future. Additionally, DeGaetano and Allen (2002) found that the rise in frequency of warm maximum and minimum temperature extremes over the past few decades were most prominent for urban locations across the country. It is worth noting that the majority of stations included in this study are rural

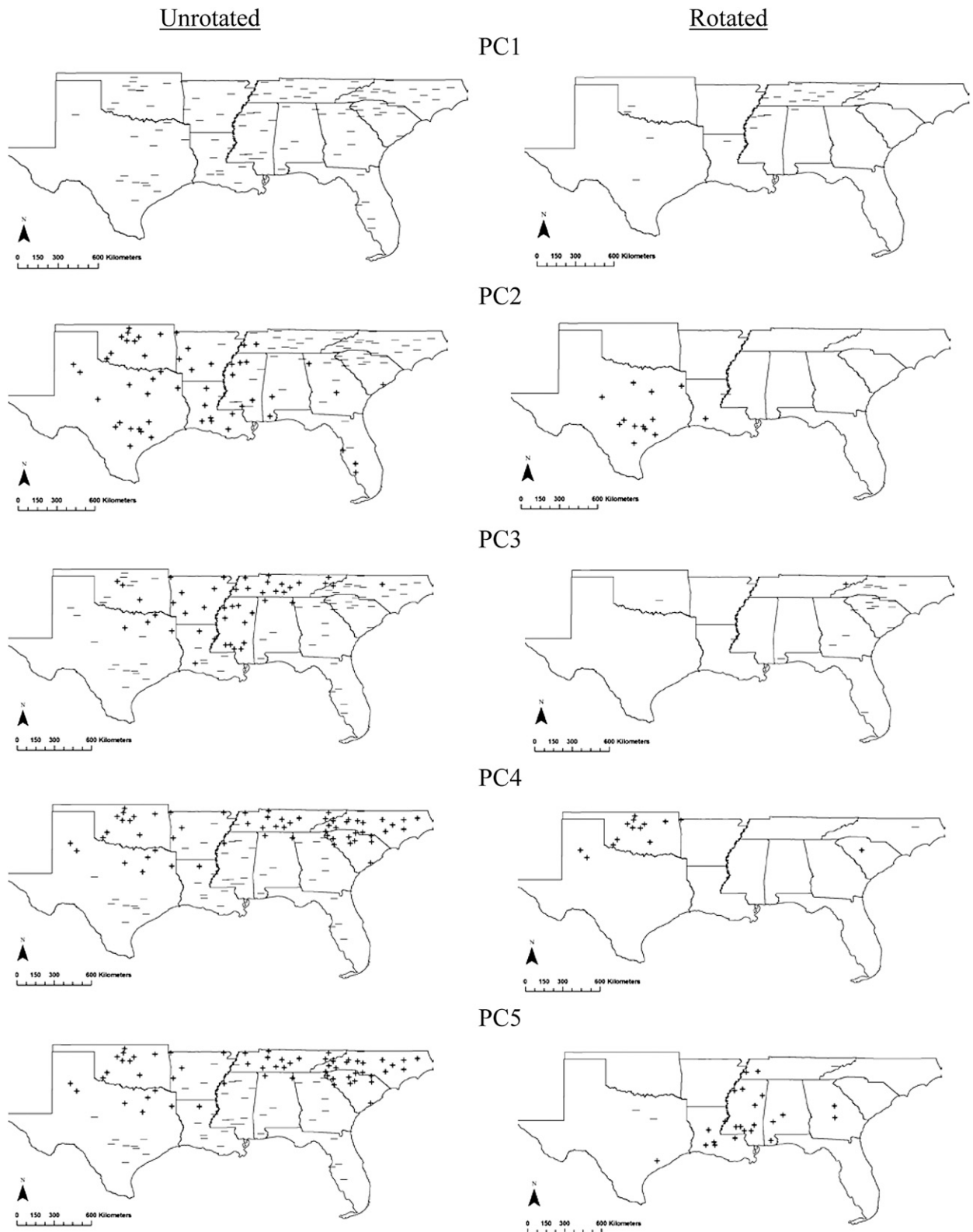


FIG. 11. Signs of the coefficients for the first five principal components, PC1–PC5, of extreme precipitation indices in the Southeast: (left) unrotated components and (right) varimax rotated components.

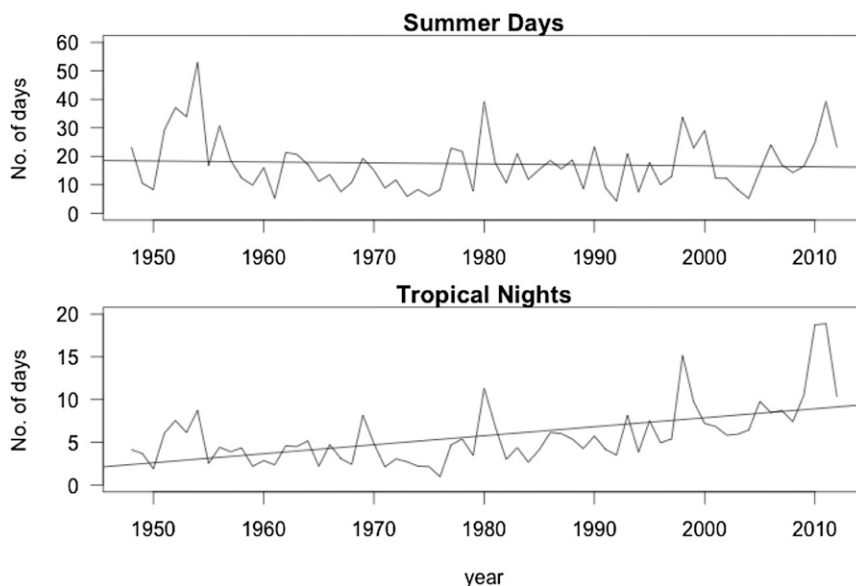


FIG. 12. Annual time series for summer days ($T_{\max} > 35^{\circ}\text{C}$) and tropical nights ($T_{\min} > 24^{\circ}\text{C}$) for the Southeast from 1948 to 2012, with the least fit trend line plotted.

locations; thus, urbanization may not be as important in driving these trends.

e. Seasonal trends

Changes in the occurrence of temperature and precipitation extremes during certain times of year can have important implications for particular sectors. Seasonal trends were investigated to provide more detail about intraannual behavior in extremes for the Southeast. Table 2 shows seasonal trends in the 13 monthly indices by state. Values reflect statewide averages for each respective 3-month season, as follows: winter (DJF), spring (MAM), summer (JJA), and fall (SON).

Extreme indices do not display a distinct seasonality for the Southeast as a whole, though some differences occur. In general, fall and summer show the greatest number of significant trends. Widespread increases in average minimum temperatures (T_{Nmean}) are evident especially in summer, as well as fall and spring. For instance, Louisiana, South Carolina, and Texas show clear warming in minimum temperatures in summer, with mostly significant trends. Significant trends in cool nights (T_{N10p}) and absolute coldest nights (T_{Nn}) are largely restricted to fall and summer. The majority of stations show downward trends in warm, maximum-related indices, particularly in winter. Widespread decreases in average maximum temperatures exist as well.

Rogers (2013) found decreasing annual, summer, and winter trends in mean air temperatures in the Southeast between 1895 and 2007. Results from this study reveal that overall decreases in mean temperatures may be

attributed mostly to decreases in mean maximum temperatures, particularly in winter. Most locations show significant decreases in diurnal temperature ranges throughout the year because of disproportionate increases in minimum versus maximum temperatures. Significant trends in minimum temperatures and diurnal temperature ranges are found especially in summer.

Fall is becoming increasingly wet regionwide, barring Florida. The maximum 1-day ($RX1\text{day}$) and consecutive 5-day ($RX5\text{day}$) precipitation indices generally display significant increases during fall, particularly for central states. Spring, summer, and winter show mixed trends in these precipitation indices, though extreme precipitation appears to have increased for many locations during summer. For instance, Alabama, Oklahoma, Florida, Mississippi, Tennessee, and Texas have become wetter in summer (with significant trends in Florida and Mississippi), while Arkansas, Louisiana, North Carolina, and South Carolina have become drier in summer (trends are generally not significant). Spring has been getting drier for most places, except Oklahoma and Tennessee.

4. Discussion and conclusions

These indices reflect increasing trends in warm and wet extremes for much of the region over this period, with drier conditions evident in South Carolina particularly. Increasing warm extremes were due to upward trends in minimum rather than maximum temperatures, and the rate at which minimum temperatures have increased appears to be outpacing any increases in

TABLE 2. Seasonal trends in average monthly indices by state from 1948 to 2012. Bold values indicate significance at the 0.05 level; italics denote significance at the 0.10 level.

		TXmean	TNmean	DTR	RX1day	RX5day	TX90p	TN90p	TX10p	TN10p	TXn	TNn	TXx	TNx
AL	fall	0.003	0.005	-0.003	0.192	0.327	-0.023	<i>0.061</i>	-0.047	-0.036	<i>0.018</i>	<i>0.016</i>	-0.006	0.010
	winter	-0.008	-0.013	0.006	0.029	-0.091	-0.059	<i>-0.072</i>	0.000	-0.005	0.006	0.019	-0.007	-0.007
	spring	0.006	0.001	0.004	-0.017	-0.172	-0.005	0.010	-0.013	-0.024	-0.004	0.004	-0.001	-0.011
	summer	-0.001	0.012	-0.013	0.066	0.111	-0.017	0.102	0.009	<i>-0.067</i>	-0.004	0.022	-0.003	0.010
AR	fall	-0.021	0.009	-0.030	0.158	0.304	-0.123	0.018	0.043	-0.080	<i>-0.023</i>	0.020	-0.019	0.000
	winter	-0.024	-0.005	-0.018	0.008	0.004	-0.068	-0.034	<i>0.062</i>	0.002	-0.012	0.026	-0.029	-0.011
	spring	-0.006	0.009	-0.016	-0.013	-0.030	-0.058	0.052	0.045	<i>-0.051</i>	-0.010	<i>0.017</i>	-0.010	-0.002
	summer	-0.009	0.014	-0.023	-0.071	-0.137	-0.087	<i>0.085</i>	<i>0.039</i>	-0.087	-0.003	0.030	-0.011	0.010
FL	fall	0.004	0.014	-0.010	-0.112	-0.226	0.008	0.103	-0.026	-0.049	0.007	0.013	0.000	0.014
	winter	-0.007	0.005	-0.013	0.040	0.074	-0.033	0.047	0.018	-0.041	-0.012	0.003	-0.003	0.014
	spring	0.000	<i>0.011</i>	-0.011	-0.048	-0.049	-0.030	0.074	-0.010	-0.077	-0.011	0.010	-0.005	0.010
	summer	0.000	0.018	-0.018	<i>0.112</i>	0.295	0.019	0.164	0.019	-0.206	-0.005	0.026	0.003	0.019
GA	fall	-0.004	0.007	-0.010	<i>0.131</i>	0.172	-0.043	<i>0.034</i>	-0.004	<i>-0.065</i>	0.012	0.023	<i>-0.013</i>	0.003
	winter	-0.010	-0.010	0.000	0.030	-0.032	-0.041	-0.101	0.021	-0.035	-0.009	<i>0.027</i>	-0.008	-0.014
	spring	-0.004	-0.001	-0.003	-0.080	<i>-0.204</i>	-0.047	-0.002	0.033	-0.032	-0.013	0.011	<i>-0.010</i>	-0.010
	summer	-0.001	0.015	-0.016	0.004	-0.030	-0.026	0.103	-0.007	-0.088	-0.005	0.032	0.001	<i>0.009</i>
LA	fall	-0.001	0.012	-0.012	0.176	0.384	-0.004	<i>0.057</i>	-0.021	-0.082	-0.008	0.017	0.001	0.010
	winter	-0.018	-0.013	-0.004	0.012	-0.069	-0.070	-0.056	0.012	-0.040	-0.003	0.023	-0.009	-0.012
	spring	0.002	0.007	-0.005	-0.094	-0.184	0.009	0.024	0.010	-0.037	-0.011	0.005	-0.004	-0.003
	summer	0.000	0.016	-0.015	-0.030	-0.023	0.000	0.153	0.008	-0.133	-0.001	0.027	0.005	0.015
MS	fall	-0.008	0.011	-0.018	0.160	0.310	-0.049	<i>0.057</i>	0.000	-0.076	-0.009	0.026	-0.009	0.010
	winter	-0.023	-0.016	<i>-0.008</i>	0.010	-0.082	-0.093	-0.098	0.029	-0.029	-0.007	<i>0.025</i>	-0.018	<i>-0.023</i>
	spring	-0.004	0.004	-0.007	-0.022	-0.163	-0.055	-0.005	<i>0.045</i>	-0.041	-0.016	0.009	-0.009	-0.010
	summer	-0.011	0.013	-0.024	0.131	0.181	-0.093	0.068	0.052	-0.109	<i>-0.018</i>	0.030	-0.010	<i>0.007</i>
NC	fall	-0.007	0.002	-0.010	0.071	0.093	-0.034	-0.009	0.024	-0.076	0.000	0.027	<i>-0.012</i>	-0.003
	winter	-0.012	-0.012	0.000	-0.017	-0.075	-0.041	-0.105	0.029	-0.055	-0.012	<i>0.024</i>	-0.003	<i>-0.021</i>
	spring	-0.007	-0.004	-0.003	0.007	-0.002	-0.024	-0.024	<i>0.050</i>	-0.024	-0.029	0.005	-0.006	-0.014
	summer	-0.002	0.013	-0.014	-0.013	-0.089	-0.015	0.072	0.003	-0.082	-0.002	0.029	-0.005	0.008
OK	fall	-0.014	-0.003	-0.012	0.119	0.153	-0.068	-0.008	0.032	-0.016	<i>-0.026</i>	0.004	-0.012	0.000
	winter	-0.008	-0.007	-0.001	0.072	<i>0.135</i>	0.000	-0.053	0.016	-0.012	0.002	0.020	-0.004	-0.033
	spring	-0.002	0.000	-0.002	0.165	0.236	-0.028	0.022	0.008	-0.016	-0.006	0.018	-0.008	0.000
	summer	-0.002	0.006	-0.007	0.057	0.126	-0.005	0.049	0.008	-0.035	0.002	0.019	-0.004	0.002
SC	fall	<i>-0.011</i>	0.010	-0.021	0.059	0.008	-0.065	0.063	0.006	-0.082	0.003	0.027	-0.023	0.005
	winter	-0.008	0.001	-0.009	-0.040	-0.093	-0.046	-0.036	-0.004	-0.054	0.002	0.028	-0.008	-0.001
	spring	0.000	0.007	-0.006	<i>-0.099</i>	-0.195	-0.018	0.043	0.007	<i>-0.055</i>	-0.010	0.010	-0.007	0.002
	summer	0.000	0.018	-0.018	-0.014	-0.044	-0.015	0.137	-0.039	-0.102	0.008	0.028	-0.004	0.014
TN	fall	-0.004	0.010	<i>-0.015</i>	0.129	<i>0.156</i>	-0.041	0.025	0.007	-0.090	0.007	0.029	<i>-0.013</i>	0.002
	winter	-0.010	-0.005	-0.005	-0.037	-0.193	-0.042	<i>-0.059</i>	0.019	-0.034	0.001	0.029	-0.009	-0.011
	spring	0.002	0.004	-0.004	0.070	0.113	0.003	0.027	0.016	-0.052	-0.010	0.004	-0.002	-0.004
	summer	-0.007	0.014	-0.021	0.025	0.085	-0.082	0.070	0.020	-0.098	-0.005	0.030	-0.010	0.006
TX	fall	-0.004	0.015	-0.019	0.049	0.084	-0.065	0.075	0.003	<i>-0.064</i>	-0.010	0.009	-0.009	0.016
	winter	-0.003	0.006	-0.010	0.064	0.073	-0.019	0.002	-0.021	-0.057	0.016	0.035	-0.007	0.004
	spring	0.005	0.016	<i>-0.011</i>	0.006	-0.040	-0.004	0.097	-0.025	-0.043	0.011	0.014	-0.003	0.014
	summer	-0.009	0.015	-0.024	0.058	0.128	-0.074	0.121	0.038	-0.111	0.003	0.024	<i>-0.013</i>	0.011

extreme maximum temperatures. If trends persist, the lack of relief at night from excessive heat may have severe public health implications, especially for vulnerable populations. The number of frost days significantly decreased for many locations, consistent with overall warming patterns. Similar results in these same temperature indices were found for New York (Insaf et al. 2012), Utah (dos Santos et al. 2011), and the Northeast (Brown et al. 2010; Griffiths and Bradley 2007). However, the strongest warming in the Northeast was

observed as decreases in frost days and increases in growing season length (GSL) (Brown et al. 2010), with some northeastern stations seeing a 2.2 days per decade increase in the GSL (Griffiths and Bradley 2007). In the Southeast, trends in the GSL have been more variable and less clear, and only 8% of stations exhibit significant trends in this index. Rather, the strongest warming was from increases in tropical nights and corresponding decreases in cool nights, consistent with other research that has found stronger increases in minimum rather than

maximum temperatures globally in the past 60 yr or so for most land areas (Alexander et al. 2006; Donat et al. 2013; Frich et al. 2002; Peterson et al. 2012).

Decreasing trends in maximum temperature-related indices are consistent with previous studies that have observed a “warming hole” over much of the eastern and southeastern regions of the United States, particularly in maximum (Donat et al. 2013) and mean (Rogers 2013) temperatures. Cooling trends have been observed in the central Great Plains (Pan et al. 2004) and Southeast (Groisman et al. 2004; Lu et al. 2005; Lund et al. 2001; Rogers 2013) during much of the twentieth century. The Southeast is one of few regions globally to not show an overall warming trend in surface temperatures over the twentieth century (Stocker et al. 2014). Minimal warming observed in the central United States has been previously associated with changes in low-level circulation patterns causing increased rainfall and replenishment of soil moisture, leading to increased summer evapotranspiration and lower daytime temperatures (Pan et al. 2004). Given that much of the Southeast experienced increasing wetness during this period, including in summer and fall, coupled with a suppression of daytime extreme temperatures, this explanation has plausibility for the broader Southeast region. Kunkel et al. (2013) summarized additional hypotheses that have been made regarding the lack of warming in the Southeast, including increased cloud cover and precipitation; increased aerosols and biogenic production; changes in sensible heat flux due to irrigation; and changes in North Atlantic and tropical Pacific sea surface temperatures.

Much of the Southeast experienced increasingly more extreme wet days during this period, particularly in far western and central areas. Increases in the frequency of heavy and very heavy precipitation days were largely restricted to western portions: namely, Texas, Oklahoma, and Louisiana. Increases in extremely wet precipitation days occurred mostly in parts of Mississippi, Tennessee, and western North Carolina. Evidence further suggests that precipitation events became more intense, with increasing magnitudes and shorter durations. These precipitation indices generally agree with previous research that found increases in precipitation extremes for eastern portions of North America (Donat et al. 2013) and much of the United States (Knight and Davis 2009; Kunkel 2003), including increasing frequency since the early 1900s (Kunkel 2003) and increases from tropical cyclones in recent decades (Knight and Davis 2009).

The strength and position of the BH likely play a role in driving the spatial variability observed in these indices. Seasonal shifts in the BH exert the strongest influence on daily temperature and precipitation in the Southeast, more so than variations in the El Niño–Southern

Oscillation (ENSO) (Henderson and Robinson 1994; Katz et al. 2003). Further, the BH index has been shown to exert the greatest influence on regional precipitation variability during all four seasons in the Southeast (Vega and Henderson 1996). Uncertainty remains, however, over how the BH may be changing and contributing to extremes. Li et al. (2012) suggest the BH has intensified in recent years, resulting in a westward shift in its western ridge in summer. Normally, its more westerly position in summer results in the transport of warm, moist air from the North Atlantic over the Southeast, increasing the probability of rainfall along the East Coast. A shift farther west than normal would bring the western edge of the BH closer to land areas of the Southeast, with areas of subsiding air closer to land inhibiting rainfall along the East Coast (Katz et al. 2003). Anticyclonic airflow associated with the BH would have a greater impact on areas farther west by bringing warm, moist air from the Gulf of Mexico over the central and western portions of the Southeast and increasing precipitation in these areas. Diem (2013) found that increased interannual variability in the western Bermuda high index (WBHI) may explain increased variance in rainfall in the Southeast. However, he hypothesized that increased atmospheric humidity is responsible for more frequent rainfall days in recent decades, rather than a shift in the western ridge of the BH.

Trends observed in this study reflect a spatial pattern consistent with that described by Li et al. (2012), whereby a westward shift in the BH may have inhibited precipitation in the east but increased instability and precipitation farther west, as reflected in the annual total wet day precipitation (Fig. 9e) and heavy precipitation days (Fig. 10a) indices and exemplified in Figs. 4 and 5. If the BH expands and shifts westward (Coleman 1988; Keim 1997), the pattern of relatively dry, more stable conditions along the East Coast and wetter conditions in the central Gulf Coast may continue. However, more research is needed to determine how the BH responds to climate change and the respective roles of the BH and atmospheric humidity in influencing extreme precipitation regimes in the region. It is important to reiterate that this analysis only reflects observed patterns over a 65-yr period from 1948 to 2012 and may not be indicative of future trends. In fact, Kunkel et al. (2013) show that mean and extreme precipitation (number of days with precipitation > 1 inch) differ from these observed trends when projected to the 2041–70 period, whereby eastern portions of the Southeast show increasing wetness and western areas (i.e., Louisiana, Arkansas, and Mississippi) show drier conditions.

This research further presented a “geography of climate extremes” for the Southeast with important subregional differences based on PCA. Temperature

extremes exhibited an east–west regionalization, from Texas and Oklahoma extending east to Mississippi and half of Tennessee, with a second region extending from Mississippi and Tennessee eastward. A precipitation PCA further subdivided the Southeast into multiple smaller regions, suggesting precipitation extremes vary greatly across the region, more than total precipitation (Henderson and Vega 1996). The majority of the variance in precipitation extremes could not be explained by just a few components, unlike temperature extremes, suggesting PCA may be less useful in describing extreme precipitation variability. This research has relevance for regional climate centers in targeting the delivery of information based on more homogeneous regions of extreme behavior, as well as helping inform development of adaptation strategies and sharing “lessons learned” across different parts of the region.

Acknowledgments. We wish to thank Dr. Jill Trepanier for her guidance in R, Dr. Melanie Gall for her guidance and overall input, and the two anonymous reviewers for their comments and suggestions that greatly improved the manuscript. We would also like to acknowledge the WMO ETCCDI, linkage project LP100200690, and CLIMDEX (<http://www.climdex.org>), which developed the indices and maintains the R source code that was used in this analysis.

REFERENCES

- Alexander, L. V., and Coauthors, 2006: Global observed changes in daily climate extremes of temperature and precipitation. *J. Geophys. Res.*, **111**, D05109, doi:[10.1029/2005JD006290](https://doi.org/10.1029/2005JD006290).
- , N. Tapper, X. Zhang, H. J. Fowler, C. Tebaldi, and A. Lynch, 2009: Climate extremes: Progress and future directions. *Int. J. Climatol.*, **29**, 317–319, doi:[10.1002/joc.1861](https://doi.org/10.1002/joc.1861).
- Brown, P. J., R. S. Bradley, and F. T. Keimig, 2010: Changes in extreme climate indices for the northeastern United States, 1870–2005. *J. Climate*, **23**, 6555–6572, doi:[10.1175/2010JCLI3363.1](https://doi.org/10.1175/2010JCLI3363.1).
- Buell, C. E., 1975: The topography of empirical orthogonal functions. *Proc. Fourth Conf. on Probability and Statistics in Atmospheric Sciences*, Tallahassee, FL, Amer. Meteor. Soc., 188–193.
- Changnon, S. A., R. A. Pielke, D. Changnon, R. T. Sylvester, and R. Pulwarty, 2000: Human factors explain the increased losses from weather and climate extremes. *Bull. Amer. Meteor. Soc.*, **81**, 437–442, doi:[10.1175/1520-0477\(2000\)081<0437:HFETIL>2.3.CO;2](https://doi.org/10.1175/1520-0477(2000)081<0437:HFETIL>2.3.CO;2).
- Coleman, J. M., 1988: Climatic warming and increased summer aridity in Florida, U.S.A. *Climatic Change*, **12**, 165–178, doi:[10.1007/BF00138937](https://doi.org/10.1007/BF00138937).
- DeGaetano, A. T., and R. J. Allen, 2002: Trends in twentieth-century temperature extremes across the United States. *J. Climate*, **15**, 3188–3205, doi:[10.1175/1520-0442\(2002\)015<3188:TITCTE>2.0.CO;2](https://doi.org/10.1175/1520-0442(2002)015<3188:TITCTE>2.0.CO;2).
- Diem, J. E., 2013: Influences of the Bermuda high and atmospheric moistening on changes in summer rainfall in the Atlanta, Georgia region, USA. *Int. J. Climatol.*, **33**, 160–172, doi:[10.1002/joc.3421](https://doi.org/10.1002/joc.3421).
- Dodge, Y., 1985: *Analysis of Experiments with Missing Data*. Wiley, 449 pp.
- Donat, M. G., L. V. Alexander, H. Yang, I. Durre, R. Vose, and J. Caesar, 2013: Global land-based datasets for monitoring climatic extremes. *Bull. Amer. Meteor. Soc.*, **94**, 997–1006, doi:[10.1175/BAMS-D-12-00109.1](https://doi.org/10.1175/BAMS-D-12-00109.1).
- dos Santos, C. A. C., C. M. U. Neale, T. V. R. Rao, and B. B. da Silva, 2011: Trends in indices for extremes in daily temperature and precipitation over Utah, USA. *Int. J. Climatol.*, **31**, 1813–1822, doi:[10.1002/joc.2205](https://doi.org/10.1002/joc.2205).
- Easterling, D. R., J. L. Evans, P. Ya. Groisman, T. R. Karl, K. E. Kunkel, and P. Ambenje, 2000: Observed variability and trends in extreme climate events: A brief review. *Bull. Amer. Meteor. Soc.*, **81**, 417–425, doi:[10.1175/1520-0477\(2000\)081<0417:OVATIE>2.3.CO;2](https://doi.org/10.1175/1520-0477(2000)081<0417:OVATIE>2.3.CO;2).
- Faiers, G. E., and B. D. Keim, 2008: Three-hour and twenty-four-hour rainstorm ratios across the southern United States. *J. Hydrol. Eng.*, **13**, 101–104, doi:[10.1061/\(ASCE\)1084-0699\(2008\)13:2\(101\)](https://doi.org/10.1061/(ASCE)1084-0699(2008)13:2(101)).
- , —, and K. K. Hirschboeck, 1994: A synoptic evaluation of frequencies and intensities of extreme three- and 24-hour rainfall in Louisiana. *Prof. Geogr.*, **46**, 156–163, doi:[10.1111/j.0033-0124.1994.00156.x](https://doi.org/10.1111/j.0033-0124.1994.00156.x).
- Frich, P., L. V. Alexander, P. Della-Marta, B. Gleason, M. Haylock, A. K. Tank, and T. C. Peterson, 2002: Observed coherent changes in climatic extremes during the second half of the twentieth century. *Climate Res.*, **19**, 193–212, doi:[10.3354/clr019193](https://doi.org/10.3354/clr019193).
- Gall, M., K. A. Borden, C. T. Emrich, and S. L. Cutter, 2011: The unsustainable trend of natural hazard losses in the United States. *Sustainability*, **3**, 2157–2181, doi:[10.3390/su3112157](https://doi.org/10.3390/su3112157).
- Green, M. C., R. G. Floccini, and L. O. Myrup, 1993: Use of temporal principal component analysis to determine seasonal periods. *J. Appl. Meteor.*, **32**, 986–995, doi:[10.1175/1520-0450\(1993\)032<0986:UOTPCA>2.0.CO;2](https://doi.org/10.1175/1520-0450(1993)032<0986:UOTPCA>2.0.CO;2).
- Griffiths, M. L., and R. S. Bradley, 2007: Variations of twentieth-century temperature and precipitation extreme indicators in the Northeast United States. *J. Climate*, **20**, 5401–5417, doi:[10.1175/2007JCLI1594.1](https://doi.org/10.1175/2007JCLI1594.1).
- Groisman, P. Ya., R. W. Knight, T. R. Karl, D. R. Easterling, B. Sun, and J. H. Lawrimore, 2004: Contemporary changes of the hydrological cycle over the contiguous United States: Trends derived from in situ observations. *J. Hydrometeorol.*, **5**, 64–85, doi:[10.1175/1525-7541\(2004\)005<0064:CCOTHC>2.0.CO;2](https://doi.org/10.1175/1525-7541(2004)005<0064:CCOTHC>2.0.CO;2).
- Hamilton, L. C., 1992: *Regression with Graphics*. Duxbury, 363 pp.
- Henderson, K. G., and P. J. Robinson, 1994: Relationships between the Pacific/North American teleconnection patterns and precipitation events in the southeastern USA. *Int. J. Climatol.*, **14**, 307–323, doi:[10.1002/joc.3370140305](https://doi.org/10.1002/joc.3370140305).
- , and A. J. Vega, 1996: Regional precipitation variability in the southern United States. *Phys. Geography*, **17**, 93–112.
- , and R. A. Muller, 1997: Extreme temperature days in the south-central United States. *Climate Res.*, **8**, 151–162, doi:[10.3354/cr008151](https://doi.org/10.3354/cr008151).
- Insaif, T. Z., S. Lin, and S. C. Sheridan, 2012: Climate trends in indices for temperature and precipitation across New York State, 1948–2008. *Air Qual. Atmos. Health*, **6**, 247–257, doi:[10.1007/s11869-011-0168-x](https://doi.org/10.1007/s11869-011-0168-x).
- Josse, J., and F. Husson, 2012: Selecting the number of components in PCA using cross-validation approximations. *Comput. Stat. Data Anal.*, **56**, 1869–1879, doi:[10.1016/j.csda.2011.11.012](https://doi.org/10.1016/j.csda.2011.11.012).
- Karhunen, J., 2011: Robust PCA methods for complete and missing data. Aalto University School of Science Department of Information and Computer Science Rep., 34 pp. [Available online

- at http://research.ics.aalto.fi/publications/bibdb2012/public_pdfs/NNW_RobustPCA.pdf]
- Katz, R. W., M. B. Parlange, and C. Tebaldi, 2003: Stochastic modeling of the effects of large-scale circulation on daily weather in the southeastern U.S. *Climatic Change*, **60**, 189–216, doi:10.1023/A:1026054330406.
- Keim, B. D., 1996: Spatial, synoptic, and seasonal patterns of heavy rainfall in the southeastern United States. *Phys. Geogr.*, **17**, 313–328.
- , 1997: Preliminary analysis of the temporal patterns of heavy rainfall across the southeastern United States. *Prof. Geogr.*, **49**, 94–104, doi:10.1111/0033-0124.00060.
- , 1999: Precipitation annual maxima as a measure of change in extreme rainfall magnitudes in the southeastern United States over the past century. *Southeast. Geogr.*, **39**, 235–245, doi:10.1353/sgo.1999.0003.
- , G. E. Faiers, R. A. Muller, J. M. Grymes III, and R. V. Rohli, 1995: Long-term trends of precipitation and runoff in Louisiana, USA. *Int. J. Climatol.*, **15**, 531–541, doi:10.1002/joc.3370150505.
- , R. A. Muller, and G. W. Stone, 2007: Spatiotemporal patterns and return periods of tropical storm and hurricane strikes from Texas to Maine. *J. Climate*, **20**, 3498–3509, doi:10.1175/JCLI4187.1.
- Klein Tank, A. M. G., F. W. Zwiers, and X. Zhang, 2009: Guidelines on analysis of extremes in a changing climate in support of informed decisions for adaptation. WMO Climate Data and Monitoring Rep. WCDMP-72, 55 pp.
- Knight, D. B., and R. E. Davis, 2009: Contribution of tropical cyclones to extreme rainfall events in the southeastern United States. *J. Geophys. Res.*, **114**, D23102, doi:10.1029/2009JD012511.
- Kunkel, K. E., 2003: North American trends in extreme precipitation. *Nat. Hazards*, **29**, 291–305, doi:10.1023/A:1023694115864.
- , and Coauthors, 2013: Regional Climate trends and scenarios for the U.S. National Climate Assessment: Part 2. Climate of the southeast U.S. NOAA Tech. Rep. NESDIS 142-2, 103 pp.
- Li, W., L. Li, M. Ting, and Y. Liu, 2012: Intensification of Northern Hemisphere subtropical highs in a warming climate. *Nat. Geosci.*, **5**, 830–834, doi:10.1038/ngeo1590.
- Lu, Q. Q., R. Lund, and L. Seymour, 2005: An update of U.S. temperature trends. *J. Climate*, **18**, 4906–4915, doi:10.1175/JCLI3557.1.
- Lund, R., L. Seymour, and K. Kafadar, 2001: Temperature trends in the United States. *Environmetrics*, **12**, 673–690, doi:10.1002/env.468.
- Malmstadt, J., K. Scheitlin, and J. Elsner, 2009: Florida hurricanes and damage costs. *Southeast. Geogr.*, **49**, 108–131, doi:10.1353/sgo.0.0045.
- Melillo, J. M., T. T. C. Richmond, and G. W. Yohe, Eds., 2014: Climate change impacts in the United States. Third National Climate Assessment, 841 pp.
- Menne, M. J., I. Durre, R. S. Vose, B. E. Gleason, and T. G. Houston, 2012: An overview of the Global Historical Climatology Network-Daily database. *J. Atmos. Oceanic Technol.*, **29**, 897–910, doi:10.1175/JTECH-D-11-00103.1.
- , C. N. Williams Jr., and R. S. Vose, cited 2013: United States Historical Climatology Network daily temperature, precipitation, and snow data. Carbon Dioxide Information Analysis Center Dataset. [Available online at <http://cdiac.ornl.gov/epubs/ndp/ushcn/ushcn.html>]
- Moberg, A., and P. D. Jones, 2005: Trends in indices for extremes in daily temperature and precipitation in central and western Europe, 1901–99. *Int. J. Climatol.*, **25**, 1149–1171, doi:10.1002/joc.1163.
- NOAA, cited 2013: Billion dollar weather/climate disasters. [Available online at <http://www.ncdc.noaa.gov/billions/>.]
- Nogueira, R. C., B. D. Keim, D. P. Brown, and K. D. Robbins, 2013: Variability of rainfall from tropical cyclones in the eastern USA and its association to the AMO and ENSO. *Theor. Appl. Climatol.*, **112**, 273–283, doi:10.1007/s00704-012-0722-y.
- NWS, cited 2012a: National Weather Service southern region headquarters. [Available online at <http://www.srh.noaa.gov/>.]
- , 2012b: National Weather Service instruction 10-1307. Operations and Services Surface Observation Program (Land) NDPD 10-13, 54 pp. [Available online at <http://www.nws.noaa.gov/directives/sym/pd01013007curr.pdf>.]
- Pan, Z., R. W. Arritt, E. S. Takle, W. J. Gutowski Jr., C. J. Anderson, and M. Segal, 2004: Altered hydrologic feedback in a warming climate introduces a “warming hole.” *Geophys. Res. Lett.*, **31**, L17109, doi:10.1029/2004GL020528.
- Peterson, T. C., P. A. Stott, and S. Herring, 2012: Explaining extreme events of 2011 from a climate perspective. *Bull. Amer. Meteor. Soc.*, **93**, 1041–1067, doi:10.1175/BAMS-D-12-00021.1.
- Pielke, R. A., J. Gratz, C. Landsea, D. Collins, M. Saunders, and R. Musulin, 2008: Normalized hurricane damage in the United States, 1900–2005. *Nat. Hazards Rev.*, **9**, 29–42, doi:10.1061/(ASCE)1527-6988(2008)9:1(29).
- Richman, M., 1986: Rotation of principal components. *J. Climatol.*, **6**, 293–335, doi:10.1002/joc.3370060305.
- Rogers, J. C., 2013: The 20th century cooling trend over the southeastern United States. *Climate Dyn.*, **40**, 341–352, doi:10.1007/s00382-012-1437-6.
- Solomon, S., D. Qin, M. Manning, Z. Chen, M. Marquis, K. B. Averyt, M. Tignor, and H. L. Miller, Eds., 2007: *Climate Change 2007: The Physical Science Basis*. Cambridge University Press, 996 pp.
- Stocker, T. F., and Coauthors, Eds., 2014: *Climate Change 2013: The Physical Science Basis*. Cambridge University Press, 1535 pp.
- Vega, A. J., and K. G. Henderson, 1996: On the use of eigenvector techniques in climatological analysis. *Pa. Geogr.*, **34**, 50–73.
- White, D., M. Richman, and B. Yarnal, 1991: Climate regionalization and rotation of principal components. *Int. J. Climatol.*, **11**, 1–25, doi:10.1002/joc.3370110102.
- Zhang, X., and F. Yang, 2004: RCLimDex (1.0) user manual. Environment Canada, 23 pp. [Available online at <http://etccdi.pacificclimate.org/RCLimDex/RCLimDexUserManual.doc>.]
- , G. Hegerl, F. W. Zwiers, and J. Kenyon, 2005: Avoiding inhomogeneity in percentile-based indices of temperature extremes. *J. Climate*, **18**, 1641–1651, doi:10.1175/JCLI3366.1.